OVERVIEW OF THE LANGLEY SUBSONIC RESEARCH EFFORT ON SCR CONFIGURATIONS

Paul L. Coe, Jr., James L. Thomas, Jarrett K. Huffman, Robert P. Weston,
Ward E. Schoonover, Jr., and Garl L. Gentry, Jr.
NASA Langley Research Center

SUMMARY

The National Aeronautics and Space Administration is currently investigating the aerodynamic characteristics of advanced aircraft concepts which are capable of cruising efficiently at supersonic speeds. These conceptual designs are representative of future generation commercial and military vehicles and incorporate wing sweeps on the order of 70° to 80°. Unfortunately, owing to the high wing sweeps, such configurations exhibit deficiencies in the area of subsonic performance, stability, and control.

The present paper summarizes recent advances achieved by the NASA Langley Research Center in the subsonic aerodynamics of highly swept-wing designs. The most significant of these advances has been the development of leading-edge deflection concepts which effectively reduce leading-edge flow separation. The improved flow attachment results in substantial improvements in low-speed performance, significant delay of longitudinal pitch-up, increased trailing-edge flap effectiveness, and increased lateral-control capability.

The paper also considers various additional theoretical and/or experimental studies which, in conjunction with continued leading-edge deflection studies, forms the basis for Langley's future subsonic research effort.

INTRODUCTION

The National Aeronautics and Space Administration is currently investigating the aerodynamic characteristics of advanced aircraf' concepts which are capable of cruising efficiently at supersonic speeds. T ,se conceptual designs are representative of future generation commercial and military vehicles and incorporate wing sweeps on the order of 70° to 80°. (See, for example, refs. 1 and 2.) Unfortunately, owing to the high wing sweeps, such configurations exhibit deficiencies in the area of subsonic performance, stability, and control. The present paper is intended to provide a brief overview of the NASA Langley subsonic research effort which is intended to eliminate or minimize these above-mentioned deficiencies.

SYMBOLS

The longitudinal data are referred to the stability system of axes with the moment reference center being located at 59.16 percent of the reference mean aerodynamic chord. The reference wing area and chord are based on the wing planform which results from extending the inboard (74°) leading-edge sweep angle and the outboard (41.457°) trailing-edge sweep angle to the model center line. (See fig. 1.)

AR	aspect ratio
b	wing span, m (ft)
C_D	drag coefficient, Drag/qS_{ref}
$C_{D,sym}$	drag coefficient of equivalent symmetric configuration (without twist or camber) at zero lift
C_L	lift coefficient, Lift/qS_{ref}
C_{L_α}	lift-curve slope, $\partial C_L/\partial\alpha$, per deg
C_l	rolling-moment coefficient, Rolling moment/$qS_{ref}b$
C_{l_β}	lateral-stability derivative, $\partial C_l/\partial\beta$, per deg
C_m	pitching-moment coefficient, Pitching moment/$qS_{ref}c$
c	local chord, m (ft)
$\bar{c}$	reference mean aerodynamic chord, m (ft)
h	height of moment reference center above ground plane, m (ft)
q	free-stream dynamic pressure, Pa (lbf/ft^2)
R_N	Reynolds number
S_{ref}	reference wing area, m^2 (ft^2)
s	leading-edge suction parameter
$\bar{s}$	streamwise distance measured from wing leading edge
α	angle of attack, deg
β	angle of sideslip, deg
Γ	geometric anhedral, deg
δ_f	trailing-edge flap deflection normal to hinge line, positive when trailing edge is down, deg
δ_{l_e}	leading-edge deflection normal to hinge line, positive when leading edge is down, deg

DISCUSSION

Figure 1 presents a three-view sketch of the Langley SCR baseline concept (ref. 3) which has served as the focal point for the research effort summarized in figure 2. It should be noted that while much of the research has been

conducted for a particular conceptual design, the results are considered to be applicable to the generic class of highly swept-wing configurations. Recent results obtained for the areas of research indicated in figure 2 are presented in detail in references 4 through 7 and are summarized herein.

Effects of Leading-Edge Devices

As is well known, the previously mentioned deficiencies in low-speed performance, stability, and control are largely attributable to the problem of leading-edge flow separation. Consequently, Langley has concentrated its subsonic research on devising a satisfactory solution to that problem. The means considered include: deflection of the leading edge in an attempt to achieve attached flow (which is discussed in the present paper) and attempts to provide a controlled flow separation with vortex flap concepts as will be discussed in subsequent papers. (See refs. 8 and 9.)

Effect of leading-edge deflection on performance.- Figure 3 presents the drag polar for the configuration with undeflected leading edges. Also presented, for purposes of comparison, are drag polars approximating the condition of fully attached flow and the condition of fully separated flow with no subsequent reattachment. Expressions for the drag polars representing these conditions are given for fully attached flow as

$$C_D = C_{D_{sym}} + C_L^2/\pi AR \tag{1}$$

and for fully separated flow as

$$C_D = C_{D_{sym}} + C_L \tan (C_L/C_{L_\alpha}) \tag{2}$$

where $C_{D_{sym}}$ represents the drag coefficient of the untwisted, uncambered, wing-body combination at zero lift. Consideration of the experimental data of figure 3 indicates that with undeflected leading edges the flow is only partially attached for the range of lift cofficients of interest, i.e., $C_L > 0.3$. Smoke and oil flow visualization studies have identified flow separation on the outboard wing panel for $\alpha > 2^\circ$ and flow separation at the wing apex and 70.5° wing crank for $\alpha > 5^\circ$.

Figure 4 presents photographs of the wind-tunnel models used to investigate leading-edge deflection concepts intended to alleviate leading-edge flow separation. The rationale for these leading-edge concepts is discussed in detail in references 4, 6, and 10. The underlying consideration, however, is simply one of attempting to align the leading edge with the incoming flow field. The figure of merit customarily selected for such studies has been the effective leading-edge suction parameter, s, which is defined as illustrated in figure 5. (See ref. 11 for additional discussion of s.) Inasmuch as this parameter is intended to serve as an indicator of total wing efficiency, it has become customary to incorporate the influence of trailing-edge flap deflection in the calculation of s. This is accomplished by determining the envelope of the drag polar for the configuration with varying trailing-edge flap deflection

as illustrated in figure 5(b). It is, of course, acknowledged that by so doing the value of s, based on the polar envelope, is greatly influenced by the effectiveness of the trailing-edge flap system.

An initial study (ref. 4) in which an attempt was made to qualitatively evaluate the leading-edge upwash has shown that, for highly swept wings, theoretical estimates of the upwash are significantly greater than experimentally observed values. The results of that study led NASA to explore a uniform 30° leading-edge deflection, where 30° was selected as it was considered to represent an average value of the upwash along the span. The initial uniform 30° deflection studied resulted from "on-site" modifications to the wind-tunnel model shown on the left in figure 4. There was an inadequate wedge fairing between the deflected leading-edge segments and the main wing structure which resulted in a short bubble separation at the shoulder of the leading-edge flap. A more recent study, in which a circular arc fairing was introduced, has been found to eliminate this problem. Figure 6 presents the values of s calculated from the polar envelopes as a function of C_L for the uniform 30° deflected leading edges with both fairings. Also shown, for purposes of comparison, are comparable results for the configuration with an undeflected leading edge. As can be seen, both of the uniform 30° leading-edge configurations provided significant increases in s when compared with the undeflected leading edge. Furthermore, the circular arc leading-edge fairing provides about 5 to 10 percent higher values of s than the wedge fairing. It must be recalled that 30° represents an average value of the leading-edge upwash, and as such, this 30° leading edge is overdeflected at inboard span locations while being underdeflected at outboard span locations.

Additional studies in which the leading-edge deflection was contoured to more nearly align the leading edge with the incoming flow along the entire span have been conducted. The particular concepts studied are referred to as the NASA continuously warped leading edge (ref. 6) and the Boeing variable camber leading edge (ref. 10). Figure 7 presents the schedule for the leading-edge deflection angle as a function of the nondimensional semispan for these concepts. Experimental values of leading-edge suction are presented as a function of C_L in figure 8 for the Boeing variable camber concept (based on the polar envelope). Also presented for purposes of comparison are the corresponding results for the NASA uniform 30° deflected leading edge. As can be seen, the Boeing variable camber leading-edge concept results in a small increase in s for a given C_L. The NASA continously warped leading edge was unfortunately tested on a model which did not incorporate a trailing-edge flap system, and hence, a direct comparison with the values of s presented for the other concepts (based on the polar envelope) is not appropriate. Furthermore, inasmuch as the Boeing variable camber design process was conducted for conditions with $\delta_f \approx 5^{\circ}$, a comparison of results for conditions with $\delta_f \approx 0^{\circ}$ is not appropriate.

In order to provide a basis for comparison and some insight into the effect of trailing-edge flaps, figure 9 presents s versus α for the configuration with the Boeing variable camber leading-edge with several values of trailing-edge flap deflection. Also presented in figure 9 is the variation of s with respect to α for the configuration with the continously warped leading edge and $\delta_f = 0^{\circ}$. As can be seen, the continuously warped leading edge results in values of s which are equivalent to those acheived with the

variable camber leading edge for a given angle of attack; however, without the trailing-edge flap system, a higher α is required to obtain a given C_L. Additional tests are planned for the NASA continuously warped leading edge in conjunction with a trailing-edge flap system. Based on the trends observed from figure 9, it is anticipated that levels of leading edge suction higher than those presently achieved are obtainable.

It should be noted that the marked reduction in leading-edge suction, which occurs with increasing angle of attack, indicates that even with the deflected leading edges, flow separation persists at higher angles of attack. This result has been confirmed by smoke flow visualization studies which showed that, for angles of attack on the order of 8° to 10°, leading-edge separation originates at the 70.5° wing crank and on the 60° swept outboard panel. Inasmuch as the leading-edge deflection outboard of the 70.5° wing crank is largely constrained by a relatively short chord, a revised leading-edge hinge line, providing an increased chord for the leading-edge segment (as suggested in ref. 4), may aid in producing attached flow. It is further anticipated that the improvement provided by the revised hinge line would be enhanced upon the elimination of the 70.5° wing crank.

Although studies have shown that a large chord Krueger flap is effective in providing attached flow on the outboard panel, such a device may be impractical. Langley Research Center is, therefore, studying outboard panel twist and sweep in conjunction with revised outboard panel leading edges in an attempt to define alternate solutions to the problem of outboard panel flow separation.

Effect of leading-edge deflection on longitudinal stability.- In addition to improved low-speed performance, leading-edge deflection would be expected to improve longitudinal stability. Experimental results are presented in figure 10 in the form of C_m versus C_L and C_m versus α. The symbols presented in figure 10 represent the onset of pitch-up for the respective conditions. As can be seen, with undeflected leading edges, the configuration exhibits a marked pitch-up characteristic for $C_L > 0.3$ or $\alpha > 5^\circ$. The onset of this pitch-up characteristic is coincident with the formation of wing apex vortices and separation of the outboard wing panel. As expected, deflecting the wing leading edge, thereby postponing the angle of attack at which leading-edge separation occurs, results in a postponement of the pitch-up characteristic. The mild but persistent pitch-up characteristic exhibited by the configuration with deflected leading edges is considered to be a result of flow separation on the outboard wing panel. While additional research is planned to define the outboard panel geometry required to further postpone this characteristic, recent studies indicate that the linearity of C_m versus C_L, as provided by the present leading-edge devices, may be satisfactory with the introduction of α-limiting concepts.

Effect of leading-edge deflection on high lift.- The influence of leading-edge deflection on trailing-edge flap effectiveness is summarized in figure 11. As would be expected, the incremental lift provided by deflecting the plain trailing-edge flap system is markedly increased by the improved flow attachment obtained through leading-edge deflection. For values of $\delta_f < 20^\circ$, the results indicate a level of trailing-edge effectiveness which is equivalent to that

predicted by simple vortex-lattice potential-flow theory (ref. 12). Although a slotted trailing-edge system may provide increased flap effectiveness for $\delta_f > 20^o$, at lower flap deflections it would not increase the lifting capability above that which is available through use of appropriate leading-edge deflection.

Effect of leading-edge deflection on lateral control.- Consistent with the increased trailing-edge flap effectiveness, figure 12 shows that leading-edge deflection also provides a marked increase in the roll control provided by the outboard ailerons. Owing to the excessively high level of effective dihedral, which accompanies highly swept wings, improved roll control is particularly critical for this class of vehicle. When considering the current 30 knot crosswind landing criteria, the present level of effective dihedral requires that the configuration achieve a lateral-control capability on the order of $C_{\ell} = 0.04$. It is anticipated that increased lateral control will result from additional studies intended to further improve the flow over the outboard wing panel.

Effect of Reynolds Number

It should be noted that the data presented in the preceding section were obtained from tests conducted for values of R_N on the order of 2.5×10^6; hence, the results may not be directly applicable to aircraft concepts which operate at values of R_N on the order of 100×10^6. An illustration of R_N effects is provided by consideration of the pressure distribution over the leading edge of the 70° swept glove of an F-111 airplane. These data were obtained during joint NASA-Air Force flight tests. Figure 13 shows the aircraft in flight and illustrates the configuration cross section at the particular span station or which the data were measured. Figure 14 presents the experimental variation of C_p with the nondimensional distance from the leading edge, $\bar{s}/c$, at values of $R_N = 20 \times 10^6$ and 40×10^6. Data obtained at $R_N = 20 \times 10^6$ indicate the presence of a vortex core passing about 3 percent aft of the leading edge. In contrast to this result, data obtained at $R_N = 40 \times 10^6$ are indicative of attached flow conditions. The preceding result serves to illustrate the need for wind-tunnel tests conducted at representative values of flight R_N.

Additional Studies and Future Plans

Although the development of leading-edge deflection concepts has been the recent emphasis of the subsonic SCR effort, other aspects of the conceptual design are being actively studied (see fig. 2). These theoretical and/or experimental studies, in conjunction with the previously discussed leading-edge deflection studies, form the basis for Langley's future subsonic research effort. This future research effort is summarized in figures 15 and 16. Highlights of various isolated research efforts are summarized in the following discussion.

Leading-edge upwash.- As mentioned in a previous section, initial attempts to qualitatively evaluate the leading-edge upwash (ref. 4) have shown that for highly swept wings, theoretical estimates of the upwash are significantly greater than experimentally observed values. In order to quantatively define

the leading-edge upwash, laser velocimeter techniques will be used to measure the flow field. It is anticipated that these studies will provide the information necessary to develop optimum leading-edge deflection concepts.

Inboard wing leading-edge sweep and hinge line.- Low-speed experimental studies (see, for example, refs. 4 and 6) have shown that flow separation originates at the mid-span wing crank. These studies have shown that, while postponed, this separation pheneomena persists even with the deflected leading-edge concepts considered to date. In an attempt to quantatively define the potential benefits of eliminating this inboard sweep break, experimental studies will be conducted with a constant sweep inboard leading edge, as sketched in figure 16. These studies will further consider a revised leading-edge hinge line, also sketched in figure 16. The revised hinge line, which is discussed in reference 4, is intended to provide an increased leading-edge flap chord outboard (where it is most needed) while reducing the chord inboard, where leading-edge deflection is less critical.

Outboard panel twist and sweep.- As noted in a previous section, providing attached flow on the 60° outboard wing panel at moderate to high angles of attack remains a challenge. Consequently, tests are planned to determine the effect of outboard panel twist and sweep on low-speed performance, longitudinal stability, and lateral control. Increased twist (washout) of the outboard panel would, of course, degrade the span-load distribution and hence would have a detrimental effect on supersonic performance. However, if all movable wing tips are considered, increased washout may be a means for promoting attached flow. Reduced sweep of the outboard panel (in contrast to increased washout) may represent a more viable solution to the problem. Recent in-house studies have indicated that reduced outboard panel sweep would not significantly degrade supersonic performance.

The intent of the above low-speed study is to determine the twist and sweep of the outboard panel (in conjunction with revised outboard panel leading-edge treatment) required to provide attached flow and to determine the magnitude of the resulting improvements in the low-speed aerodynamic charactersitics so that a detailed trade study can be conducted.

Outboard vertical-fin position and orientation.- A theoretical study presented in reference 7 has shown that increasing the inwardly directed load on the outboard vertical fin results in an improved span-load distribution, and therefore, improved low-speed performance. The study has shown that such an increase in load may be accomplished by moving the outboard vertical fin forward or by toeing the vertical fin inwardly. Inasmuch as the present position and orientation of the outboard vertical fin is based on supersonic performance considerations, such changes may be inappropriate. However, an alternate means of increasing the vertical fin load would be to produce an effective camber surface by introducing a vertical fin rudder. Such a system may also require some form of vertical fin leading-edge treatment to prevent flow separation. Wind-tunnel tests are planned to determine if the improvement in low-speed performance predicted by theory can be achieved.

Geometric anhedral.- As noted in a previous section, the excessively high level of effective dihedral, which is associated with high wing sweep, is found

to require relatively high levels of lateral control to meet the current 30 knot crosswind landing criteria. These values of C_{l_β}, however, are based on test data for the cruise shape wing. Recent structural analysis has shown that in the landing condition the wing assumes a shape which is somewhat different from the cruise shape. The difference in wing shape results in the configuration having an increased geometric anhedral for the landing condition.

Recent wind-tunnel tests (see ref. 6) have determined the variation of C_{l_β} with respect to geometric anhedral and have further shown that the increment in C_{l_β} due to anhedral can be approximated with the use of simple vortex-lattice theory (see fig. 17). Based on the anticipated shape of the wing in the landing condition, and the results obtained from reference 5, it is considered that the values of C_{l_β} (as predicted by wind-tunnel tests of the cruise shape wing) are about 10 percent high. This value will be refined with subsequent wind-tunnel tests of the configuration employing the assumed landing geometry.

Leading-edge optimization for high-lift condition.- As noted previously, the NASA continuously warped leading edge has provided higher levels of leading-edge suction than the other concepts considered. However, this concept was tested on a model which did not incorporate trailing-edge flaps, and hence, its high-lift characteristics are not well defined. Experimental studies will be conducted for the continuously warped leading edge in conjunction with a trailing-edge flap system. Preliminary evidence indicates that the increased circulation provided by the trailing-edge flap system may require the leading-edge deflection schedule to be optimized as a function of trailing-edge flap deflection.

Ground effects.- Recent studies of ground effects (ref. 5), conducted using a vortex-lattice theoretical model (with ground-plane image) and experimentally with a moving ground belt, have shown that the configuration, as expected, experiences an increase in lift, a reduction in induced drag, and an increase in longitudinal stability when in ground effect (see fig. 18). The study has shown that the effects are generally more pronounced than previous estimates had indicated and result in a greater reduction in vertical descent rate than initially anticipated. The study, however, did not address the possible power-induced effects and, as such, remains incomplete. Current plans include additional tests to define the influence of thrust on ground effects while simultaneously exploring the magnitude and extent of the trailing vortex phenomena as it exists for the present SCR concept.

Reynolds number effects.- Limited available data indicate that significant Reynolds number effects may exist for highly swept wing concepts. Langley Research Center is, therefore, in the process of defining a highly swept wing, general research model capable of being tested at values of R_N on the order of 100×10^6 and a corresponding Mach number of 0.3. These tests will be possible in the National Transonic Facility and are tentatively scheduled for 1982.

CONCLUDING REMARKS

The present paper has been intended to briefly summarize recent advances achieved by the NASA Langley Research Center in the subsonic aerodynamics of low-aspect-ratio, highly swept-wing designs. The most significant of these advances has been the development of leading-edge deflection concepts which effectively reduce leading-edge flow separtion. The improved flow attachment results in substantial improvements in low-speed performance, significant delay of longitudinal pitch-up, increased trailing-edge flap effectiveness, and increased lateral-control capability.

The paper also considers various additional theoretical and/or experimental studies which, in conjunction with the continued leading-edge deflection studies, forms the basis for Langley's future subsonic research effort.

REFERENCES

1. Robins, A. Warner; Morris, Odell A.; and Harris, Roy V., Jr.: Recent Results in the Aerodynamics of Supersonic Vehicles. J. Aircraft, vol. 3, 1966, pp. 573-577.

2. Robins, A. Warner; Lamb, Milton; and Miller, David S.: Aerodynamic Characteristics at Mach Numbers of 1.5, 1.8, and 2.0 of a Blended Wing-Body Configuration With and Without an Integrand Canard. NASA TP 1427, 1979.

3. Staff, Hampton Technical Center, LTV Aerospace Corporation: Advanced Supersonic Technology Concept Study Reference Characteristics. NASA CR 132374, 1973.

4. Coe, Paul L., Jr.; and Weston, Robert P.: Effects of Wing Leading-Edge Deflection on the Low-Speed Aerodynamic Characteristics of a Low-Aspect-Ratio Highly Swept Arrow-Wing Configuration. NASA TP 1434, 1979. (Supercedes NASA TM 78787, 1978.)

5. Coe, Paul L., Jr.; and Thomas, James L.; Theoretical and Experimental Investigation of Ground Induced Effects for a Low-Aspect-Ratio Highly Swept Arrow-Wing Configuration. NASA TP 1508, 1979. (Supercedes NASA TM 80041, 1979.)

6. Coe, Paul L., Jr.; and Huffman, Jarrett K.: Influence of Optimized Leading-Edge Deflection and Geometric Anhedral on the Low-Speed Aerodynamic Characteristics of a Low-Aspect-Ratio Highly Swept Arrow-Wing Configuration. NASA TM 80083, 1979.

7. Johnson, Vicki S.; and Coe, Paul L., Jr.: Effect of Outboard Vertical Fin Position and Orientation on the Low-Speed Aerodynamic Performance of Highly Swept Wings. NASA TM 80142, 1979

8. Rao, D. M.: Exploratory Subsonic Investigation of Vortex-Flap Concept on Arrow Wing. Supersonic Cruise Research '79, NASA CP-2108, 1980. (Paper no. 4 of this compilation.)

9. Runyan, L. J.; Middleton, W. D.; and Paulson, J. A.: Wind Tunnel Test Results of a New Leading Edge Flap Design for Highly Swept Wings--A Vortex Flap. Supersonic Cruise Research '79, NASA CP-2108, 1980. (Paper no. 5 of this compilation.)

10. Paulson, J. A.; Boctor, M. L.; Maier, R. E.; Middleton, W. D.; and Vachal, J. D.: Leading-Edge Flap Design for an Arrow-Wing Configuration. NASA CR 145273, 1978.

11. Henderson, William P.: Studies of Various Factors Affecting Drag Due to Lift at Subsonic Speeds. NASA TN D-3584, 1966.

12. Tulinius, J.: Unified Subsonic, Transonic, and Supersonic NAR Vortex Lattice. Rep. TFD-72-253, Rockwell International Corporation, 1972

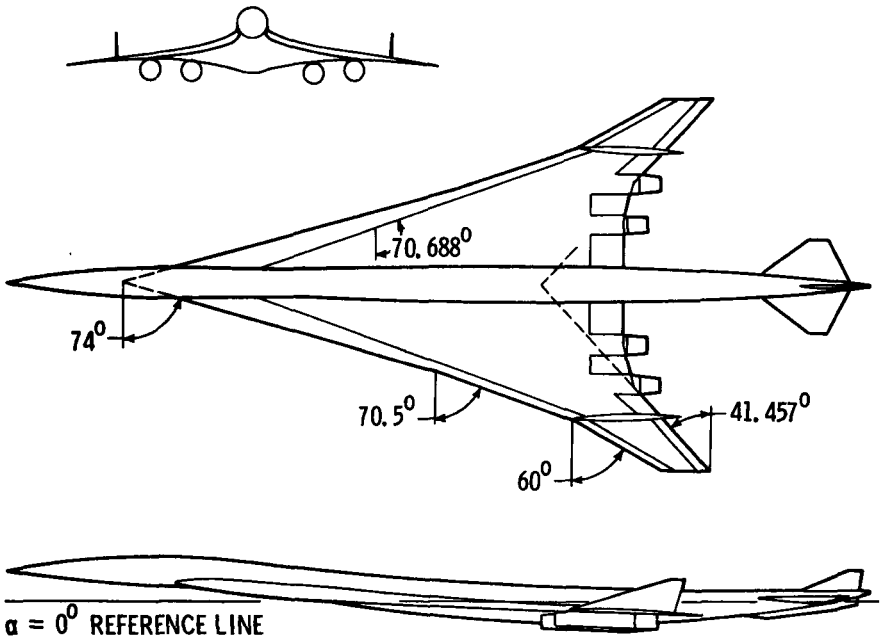

Figure 1.- Three-view sketch of Langley SCR baseline concept.

RESEARCH AREAS	PERFORMANCE	LONGITUDINAL STABILITY	HIGH LIFT	LATERAL STABILITY	LATERAL CONTROL
	OPPORTUNITIES FOR IMPROVEMENT				
• LEADING-EDGE DEVICES	X	X	X		X
- ATTACHED FLOW					
- VORTEX FLAP CONCEPTS					
• OUTBOARD PANEL TWIST AND SWEEP	X	X			X
• OUTBOARD VERTICAL FIN POSITION AND ORIENTATION	X				
• GEOMETRIC ANHEDRAL				X	
• GROUND EFFECTS	X	X			

Figure 2.- Summary of the NASA-LRC subsonic SCR program.

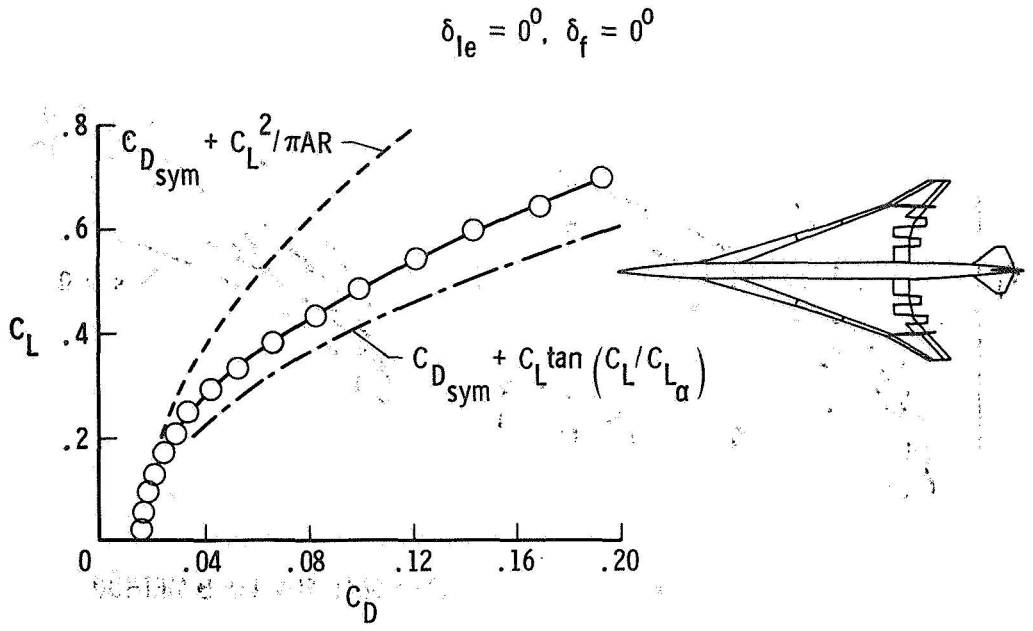

Figure 3.- Drag polar for baseline configuration.

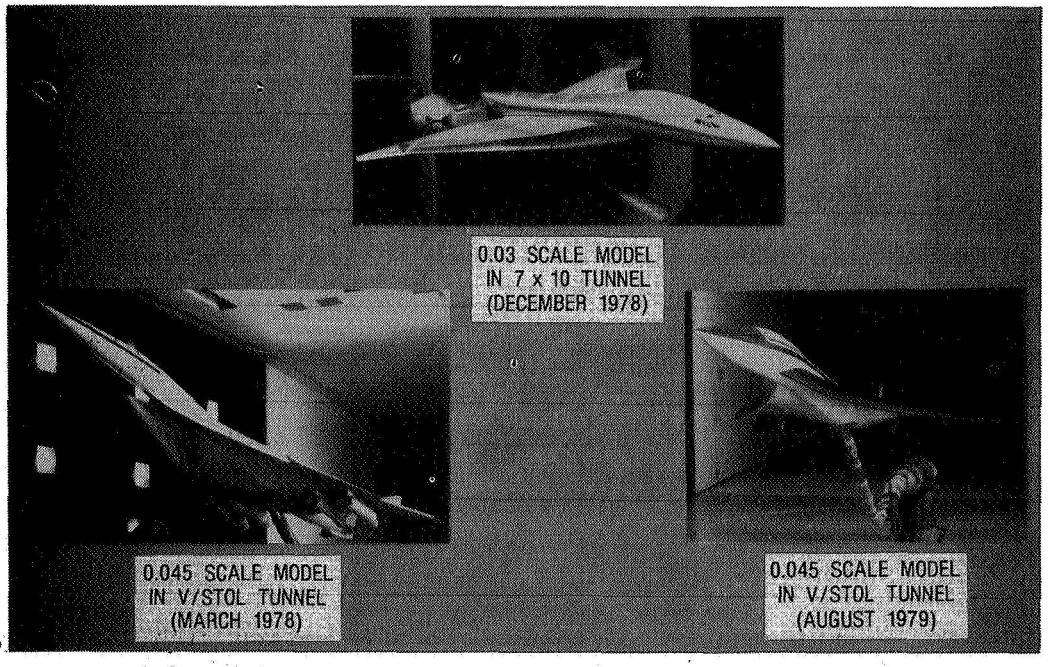

Figure 4.- Photographs of models used in leading-edge deflection studies.

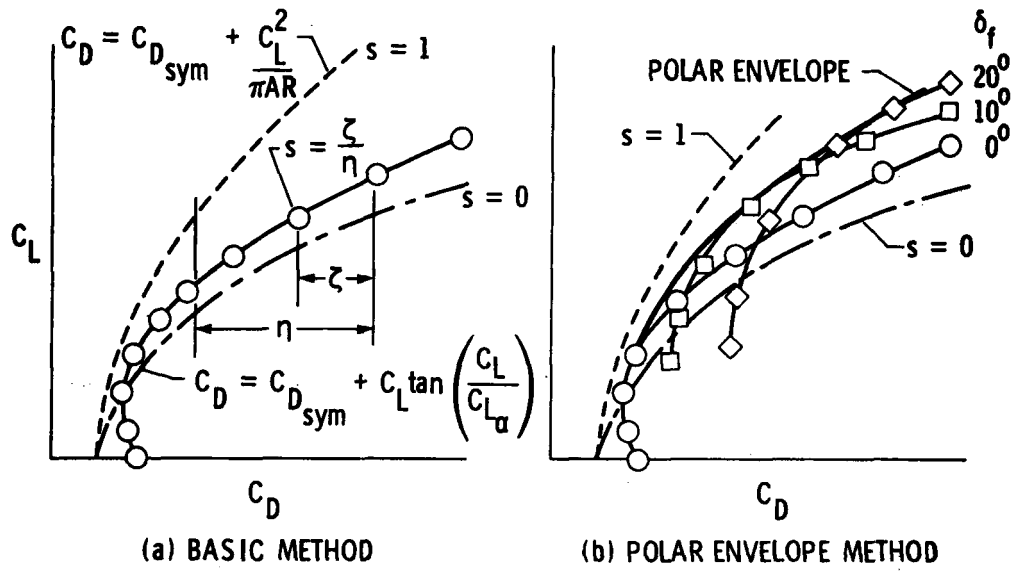

Figure 5.- Illustration of leading-edge suction determination.

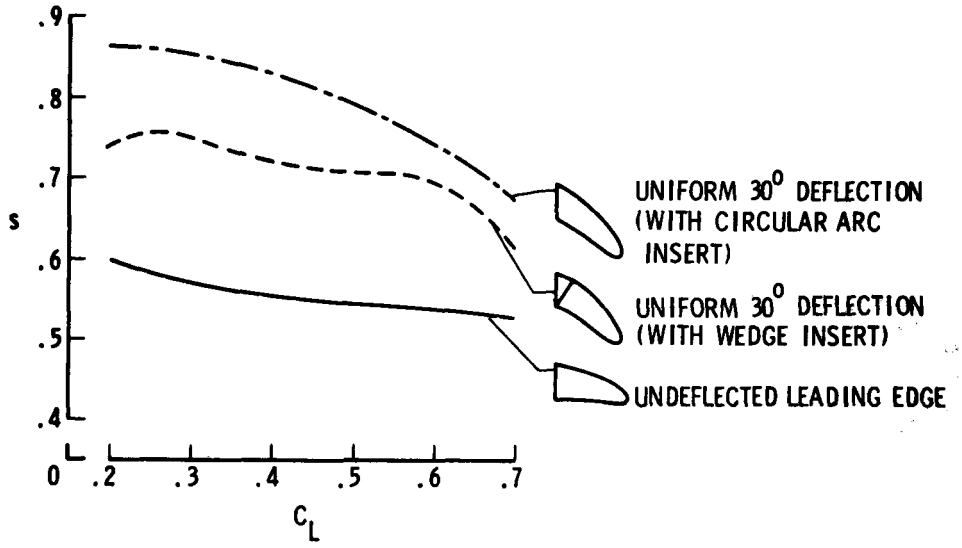

Figure 6.- s versus C_L for baseline configuration with uniformly deflected leading edge. (Polar envelope method.)

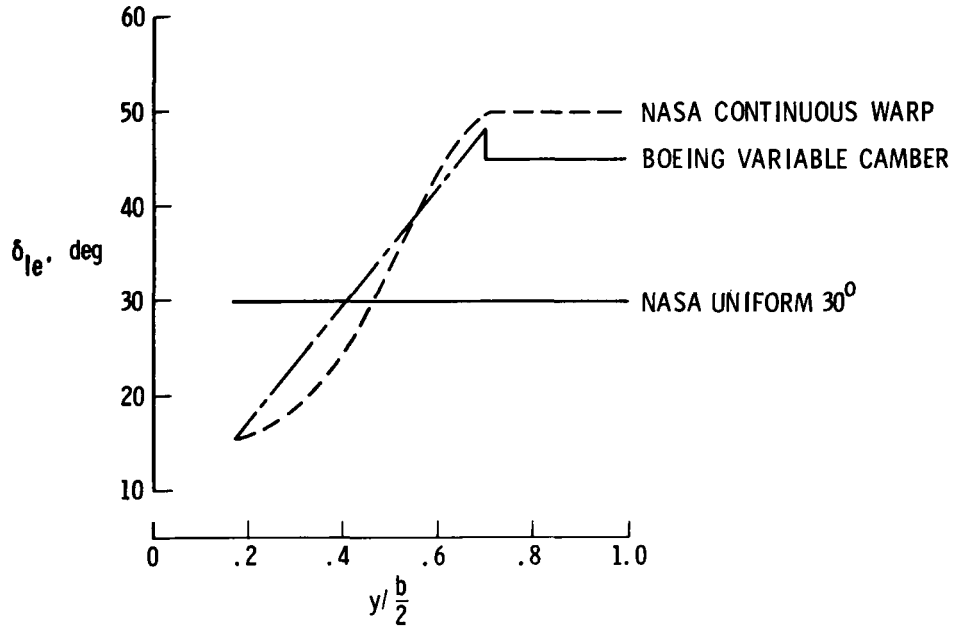

Figure 7.- Leading-edge deflection schedule for concepts studied.

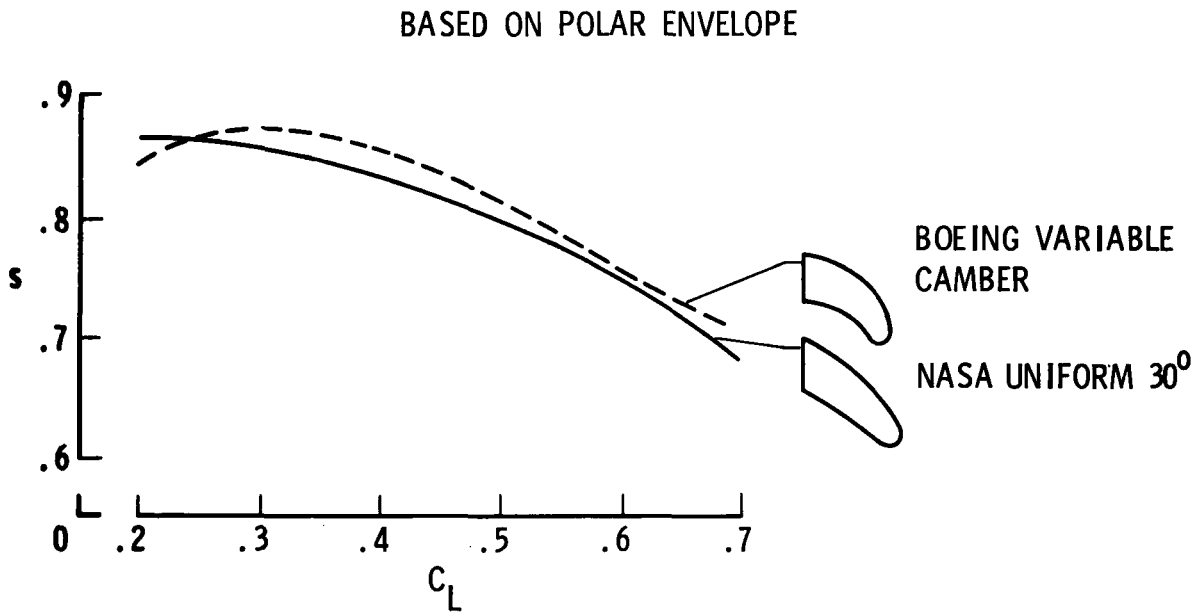

Figure 8.- s versus C_L for configuration with uniformly deflected leading edge and Boeing variable camber leading edge.

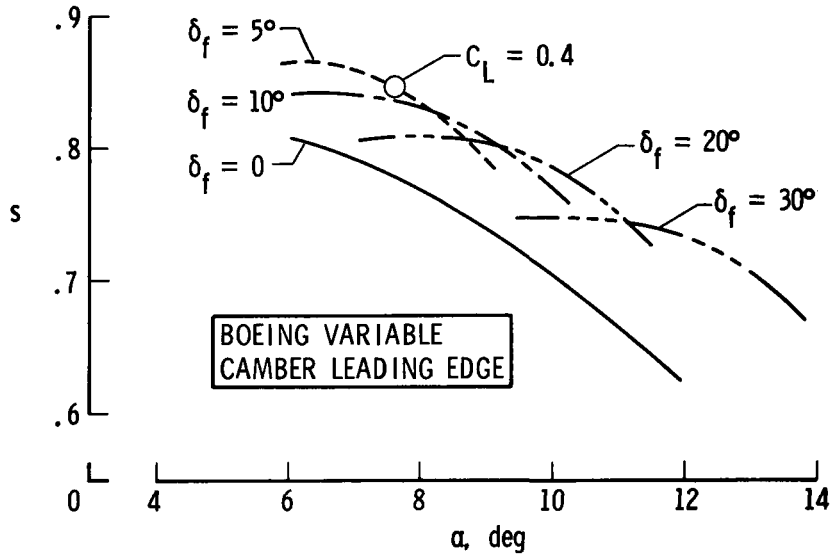

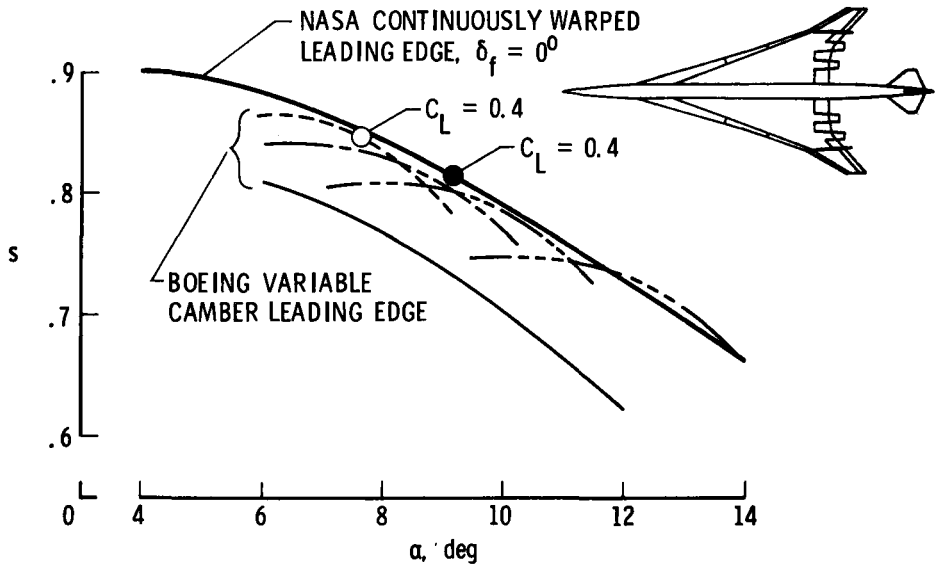

Figure 9.- Comparison of leading-edge suction for Boeing variable camber and NASA continuously warped leading edges.

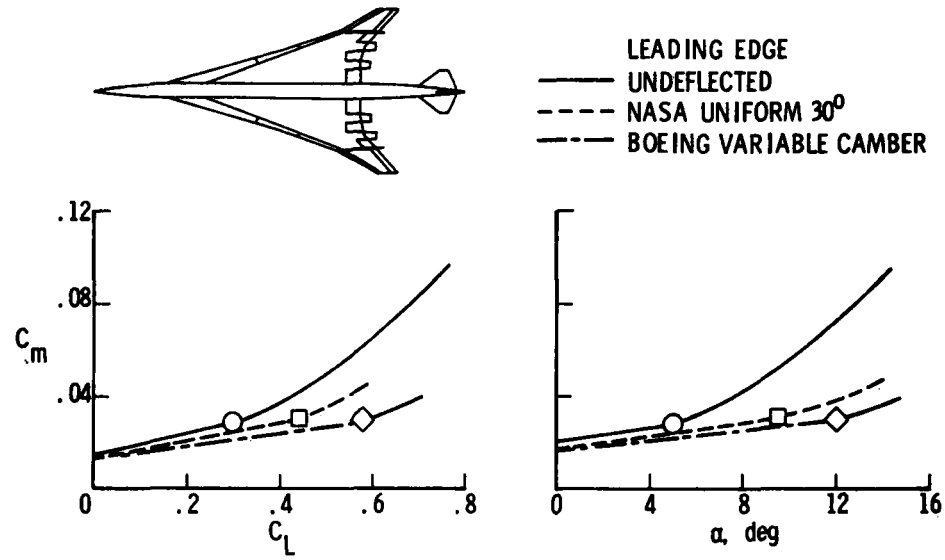

Figure 10.- Effect of leading-edge deflection on longitudinal stability. (Symbols represent the onset of pitch-up.)

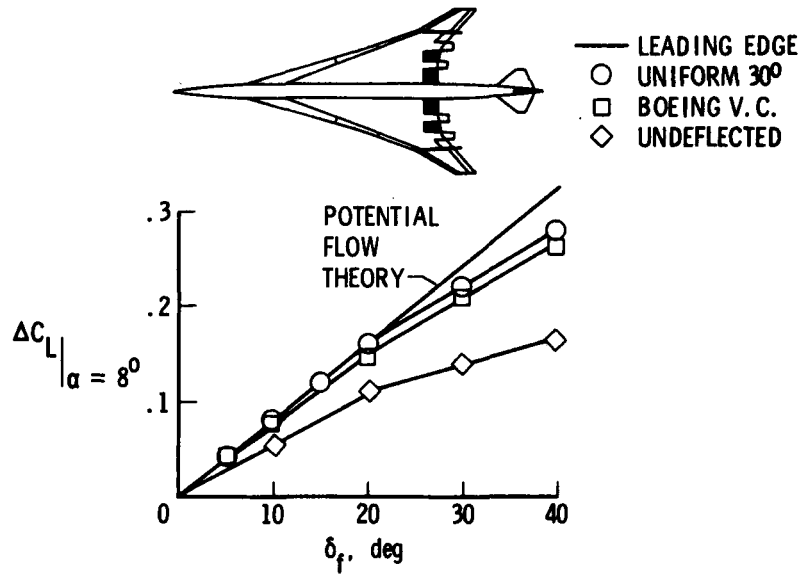

Figure 11.- Effect of leading-edge deflection on trailing-edge flap effectiveness.

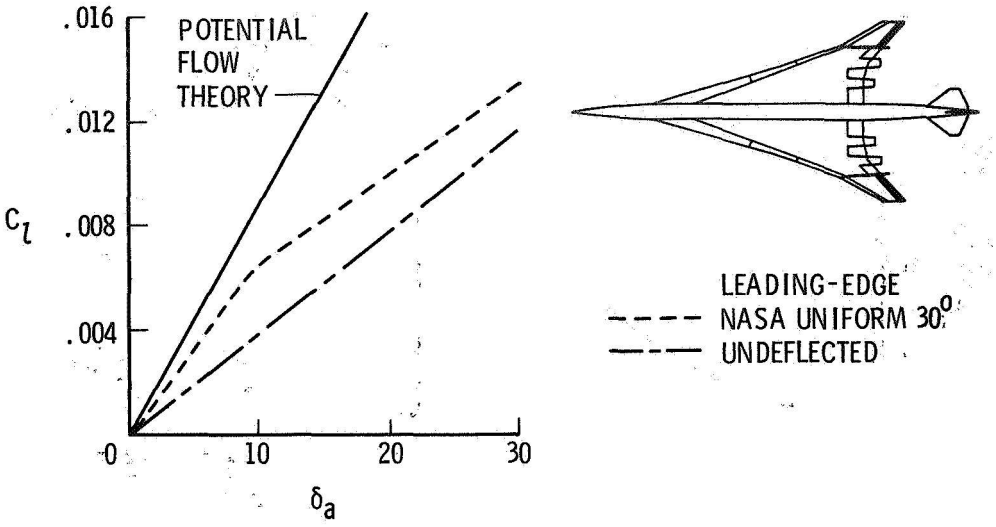

Figure 12.- Effect of leading-edge deflection on aileron effectiveness.

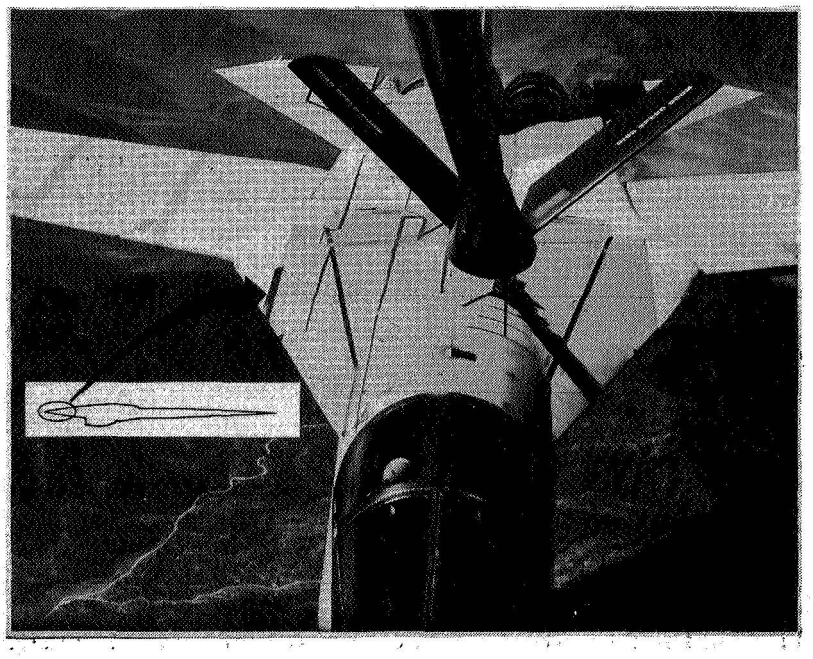

Figure 13.- F-111 during joint NASA-Air Force flight tests.

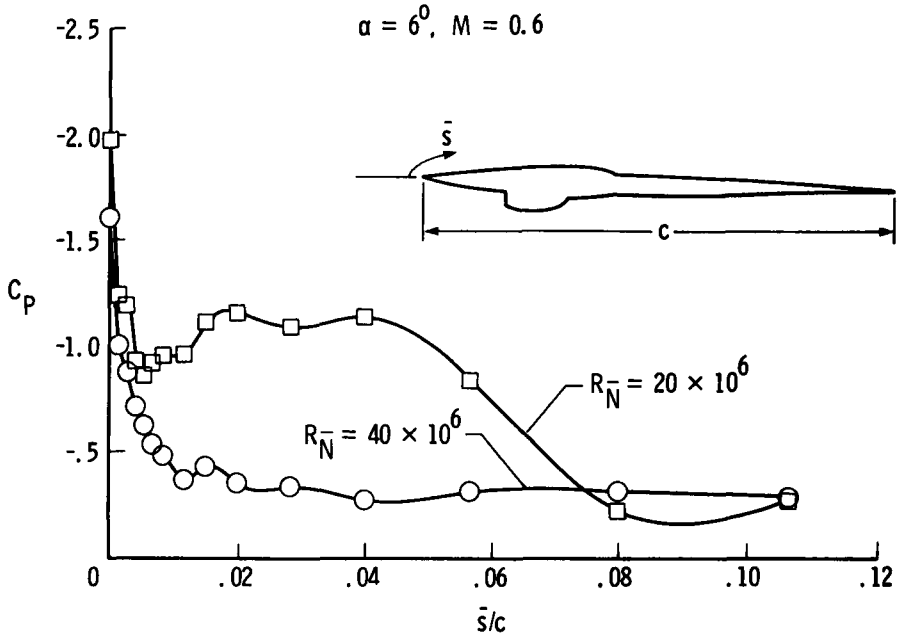

Figure 14.- Influence of R_N on leading-edge pressure distribution.

- DETERMINE LEADING EDGE UPWASH USING L.V. TECHNIQUES
- DETERMINE AERODYNAMIC IMPROVEMENTS WITH MODIFIED GEOMETRY
- OPTIMIZE LEADING EDGE FOR HIGH-LIFT CONDITION
- DETERMINE INFLUENCE OF THRUST ON GROUND EFFECTS
- DEFINE TRAILING VORTEX PHENOMENON
- DETERMINE R_N EFFECTS

Figure 15.- Summary of NASA-LRC future subsonic research effort.

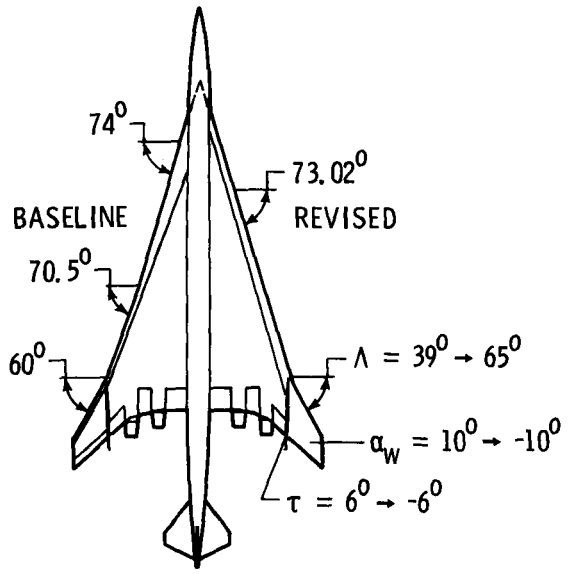

CONCEPT STUDIES

INBOARD WING

- LEADING EDGE SWEEP
- LEADING EDGE HINGE LINE

OUTBOARD WING PANEL

- TWIST
- SWEEP
- CAMBERED LEADING EDGE

OUTBOARD VERTICAL FIN

- TOE ANGLE

Figure 16.- SCR concept modification studies.

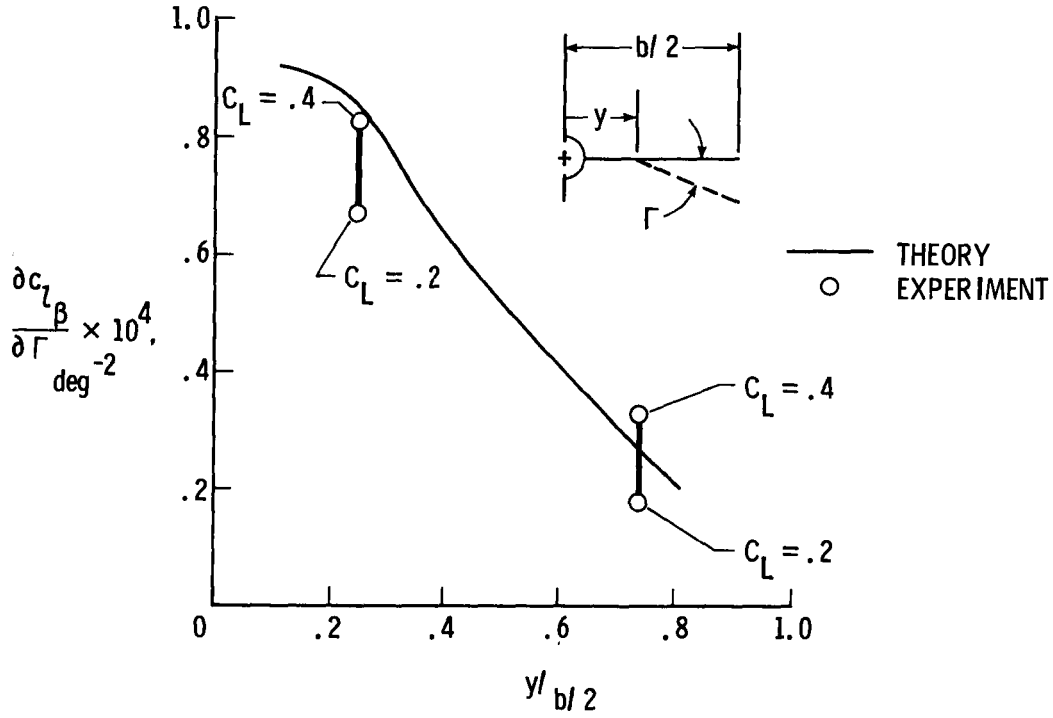

Figure 17.- Values for $\partial C_{l_\beta}/\partial \Gamma$ obtained by inclusion of additional geometric anhedral at span station $\frac{y}{b/2}$.

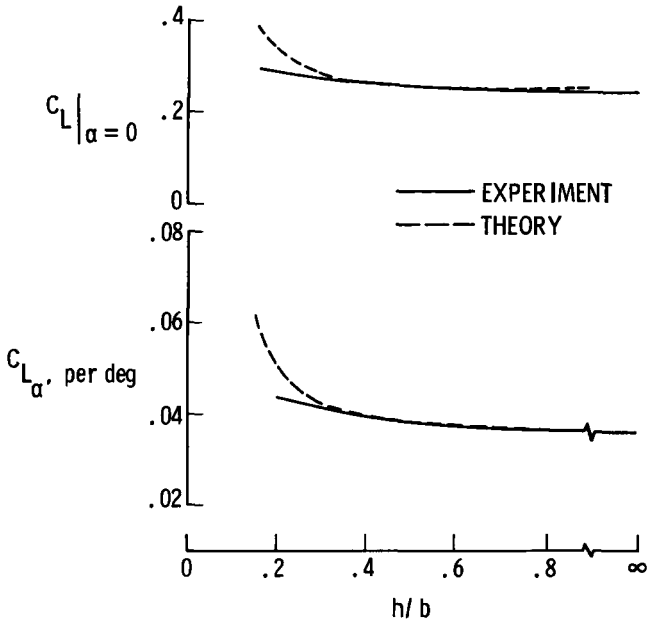

(a) Influence of ground effects on $C_L\big|_{\alpha=0}$ and C_{L_α}.

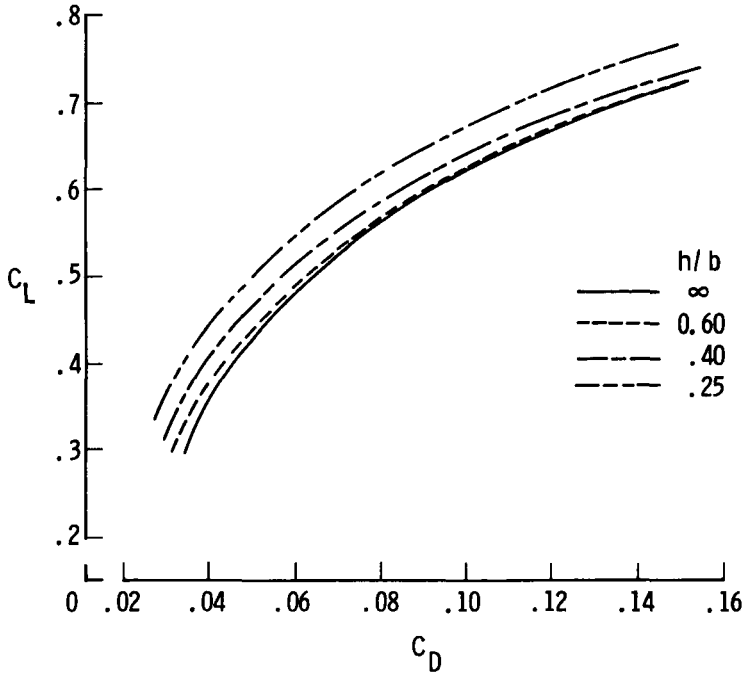

(b) Influence of ground effects on drag polar.

Figure 18.- Influence of ground effects on longitudinal aerodynamic characteristics. $\delta_f = 20^o$; $\delta_{LE} = 30^o$.

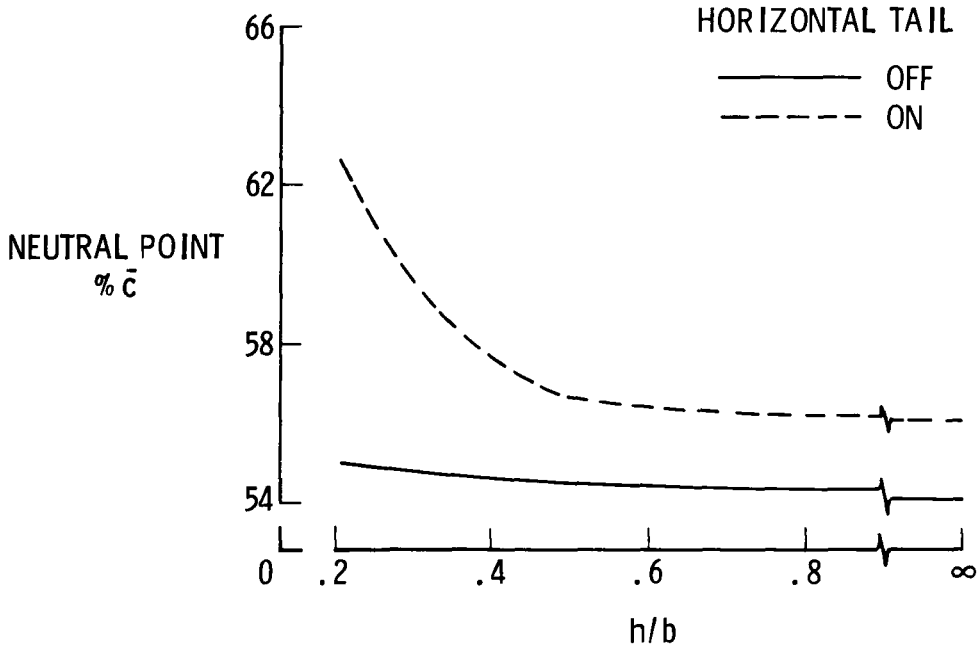

(c) Influence of ground effects on longitudinal stability.

Figure 18.- Concluded.